JNeurosci
THE JOURNAL OF NEUROSCIENCE

Research Articles: Cellular/Molecular

Activation of PERK elicits memory impairment through inactivation of CREB and downregulation of PSD95 following Traumatic Brain Injury

Tanusree Sen[1], Rajaneesh Gupta[2], Helen Kaiser[2] and Nilkantha Sen[1]

[1]*University of Pittsburgh, Department of Neurological Surgery, 200 Lothrop Street, A504, Pittsburgh, PA 15213*
[2]*Augusta University, Department of Neuroscience and Regenerative Medicine, Augusta, GA, 30907*

DOI: 10.1523/JNEUROSCI.2343-16.2017

Received: 21 July 2016

Revised: 20 April 2017

Accepted: 2 May 2017

Published: 17 May 2017

Author contributions: T.S., R.G., H.K., and N.S. performed research; T.S., R.G., H.K., and N.S. analyzed data; R.G. contributed unpublished reagents/analytic tools; N.S. designed research; N.S. wrote the paper.

We would like to acknowledge NIH funding support (RO1NS094516 and RO1EY025622) for providing support to N.S, and R.G. We would also like to thank Dr. Alexis Stranahan from the Augusta University for providing generous help to carryout DiI staining to study the synaptic morphology.

Corresponding author: senn@pitt.edu

Cite as: J. Neurosci ; 10.1523/JNEUROSCI.2343-16.2017

Activation of PERK elicits memory impairment through inactivation of CREB and downregulation of PSD95 following Traumatic Brain Injury

PERK phosphorylates CREB and PSD95

Tanusree Sen[1], Rajaneesh Gupta[2], Helen Kaiser[2], Nilkantha Sen[1,*]

[1]University of Pittsburgh, Department of Neurological Surgery
200 Lothrop Street, A504, Pittsburgh, PA 15213
[2]Augusta University, Department of Neuroscience and Regenerative Medicine
Augusta, GA, 30907

*Corresponding author: senn@pitt.edu

Abstract

The PKR-like ER kinase (PERK) a transmembrane protein resides in the endoplasmic reticulum (ER) and activation of PERK serve as a key sensor of ER-stress which has been implicated in Traumatic Brain Injury (TBI). The loss of memory is one of the most common symptoms following TBI; however, the precise role of PERK activation in memory impairment after TBI has not been well elucidated. Here we have shown that blocking the activation of PERK using GSK2656157 prevents the loss of dendritic spines and rescues memory deficits following TBI. To elucidate the molecular mechanism, we found that activated PERK directly phosphorylates CREB and PSD95 at S129 and T19 residues respectively. Phosphorylation of CREB protein prevents its interaction with a coactivator CBP and subsequently reduces BDNF level following TBI. On the other hand, phosphorylation of PSD95 leads to its downregulation in pericontusional cortex after TBI in male mice. Treatment with either GSK2656157 or overexpression of a kinase-dead mutant of PERK (PERK-K618A) rescues BDNF and PSD95 levels in the pericontusional cortex by reducing phosphorylation of CREB and PSD95 proteins following TBI. Similarly, administration of either GSK2656157 or overexpression of PERK-K618A in primary neurons rescues the loss of dendritic outgrowth and number of synapses after treatment with a PERK activator, tunicamycin. Thus, our study suggests that inhibition of PERK phosphorylation could be a potential therapeutic target to restore memory deficits following TBI.

Significance statement: TBI is the leading cause of death and disability around the world and it affects 1.7 million Americans each year. Here we have shown that TBI-activated PERK is responsible for memory deficiency which is the most common problem in TBI patients. A majority of PERK's biological activities have been attributed to its function as an eIF2α kinase. However, our study suggests that activated PERK mediates its function via increasing phosphorylation of CREB and PSD95 following TBI. Blocking PERK phosphorylation rescues spine loss and memory deficits independent of phosphorylation of eIF2α. Thus our study suggests that CREB and PSD95 are novel substrates of PERK and inhibition of PERK phosphorylation using GSK2656157 would be beneficial against memory impairment following TBI.

Introduction

Traumatic Brain Injury (TBI) is a major cause of morbidity and mortality and affects more than 1.7 million people throughout the USA annually (Nortje and Menon, 2004; Rondina et al., 2005). TBI is a contributing factor to a third (30.5%) of all injury-related deaths in the USA. Endoplasmic reticulum (ER) stress has recently received increased attention in the pathogenesis of various neurodegenerative disorders including TBI (Larner et al., 2006; Truettner et al., 2007; Begum et al., 2013; Begum et al., 2014; Logsdon et al., 2014).

Protein kinase-like endoplasmic reticulum kinase (PERK) is an eIF2α kinase and transmembrane protein resident in the endoplasmic reticulum (ER) membrane that couples ER stress signals to translation inhibition (Marciniak et al., 2006; Banhegyi et al., 2007; Saito et al., 2011; Pereira et al., 2013; Liu et al., 2015). ER stress increases the activity of PERK, which then phosphorylates eIF2α to promote reduced translation (Vattem and Wek, 2004; Wek and Cavener, 2007; Saito et al., 2011; Liu et al., 2015). PERK is one of at least four eIF2α protein kinases that include the heme-regulated kinase (HRI), the interferon-inducible, RNA-dependent protein kinase (PKR), and GCN2. Among these, only PERK function is required for the cellular response to ER stress (Saito et al., 2011; Liu et al., 2015). Phosphorylation of PERK at Thr980 within the kinase activation loop is essential for the autocatalytic activity of the kinase (Harding et al., 1999).Treatment with GSK2656157 has been shown to inhibit phosphorylation of PERK protein both *in vitro* and *in vivo* (Moreno et al., 2013; Krishnamoorthy et al., 2014).

Cyclic AMP Response Element Binding protein (CREB) is a transcription factor that binds the cyclic AMP response element (CRE) and activates transcription of several memory-related genes including BDNF. Activation of CREB is dependent upon the phosphorylation of serine 133 and interaction with a transcriptional coactivator CREB binding protein (CBP) (Ginty et al., 1994; Bonni et al., 1995; Finkbeiner et al., 1997). However, phosphorylation of CREB at S129 leads to an attenuation of its transcriptional activity, although the mechanism has not been well elucidated (Wang et al., 2010). PSD-95 is an abundant scaffold protein in the postsynaptic density (PSD) of excitatory synapses (Kim and Sheng, 2004; Cheng et al., 2006). Activation of GSK3β phosphorylates PSD95 at threonine 19 that leads to destabilization of PSD-95 in spines (Nelson et al., 2013).

In the present study, we have shown that an increase in phosphorylation of PERK inactivates CREB and causes the loss of protein level of PSD95 that collectively contributes to the memory impairment following TBI. Manipulation of PERK phosphorylation mitigates synapse loss and improve memory functions by rescuing phosphorylation levels of CREB and PSD95 both *in-vivo* and *in-vitro*.

Materials and Methods:

Drugs: GSK2656157 was purchased from Calbiochem, US and was dissolved in DMSO. DMSO was delivered by intraperitoneal injection to sham and TBI groups of mice. GSK2656157 (50 mg/kg) was delivered by intraperitoneal (i.p.) injection to sham and TBI groups at 30 min after TBI, followed by a daily dose for 24 days. Since GSK2656157 was dissolved in DMSO, only sham and TBI mice received DMSO as controls. For the experiment related to dose dependent study, we administered GSK2656157 at various doses eg, 10, 20 and 50mg/kg at 30 min after TBI, followed by a daily dose for 24 days. Mice were treated with lithium (5 mg/kg) for 24 days with or without administration of GSK2656157 (50 mg/kg) following either sham or TBI procedures (Fig. 1). We have used male mice throughout all the experiments. Then biochemical analysis was done on the 25th day (Fig. 1A). In other experiments, the mice were trained for MWM test for 6 days after completion of GSK2656157 treatment of TBI mice and the probe trial was done on the 31st day of TBI (Fig. 1B). The same sets of mice were used to monitor the synaptic density of TBI or sham mice on the 31st day following TBI. In Fig. 1C, either PERK or PERK-K618A was overexpressed in mice brain 7 days before TBI. Then biochemical analysis was performed on the 25th day after TBI. The procedure for TBI and overexpression of PERK/PERK-K618A were described in the following section.

TBI procedures: The Committee on Animal Use for Research and Education at the Augusta University approved all animal studies, in compliance with NIH guidelines. The procedure was done based on our previously published protocol (Farook et al., 2013; Kapoor et al., 2013; Sen and Sen, 2016). Briefly, adult male C57BL/6 (Jackson Laboratory), mice were anesthetized with xylazine (8 mg/kg)/ketamine (60 mg/kg) and subjected to a sham injury or controlled cortical impact. Briefly, mice were placed in a stereotaxic frame (Ambient Instruments, Richmond, VA, USA) and a 3.5 mm craniotomy was made in the right parietal bone midway between bregma and lambda with the medial edge lateral to the midline, leaving the dura intact. Mice were impacted at 4.5 m/s with a 20-ms dwell time and 1.2-mm depression using a 3-mm-diameter convex tip, mimicking a moderate TBI. Sham-operated mice underwent the identical surgical procedures but were not impacted. The incision was closed with VetBond and mice were allowed to recover. Body temperature was maintained at 37 °C using a small animal temperature controller throughout all procedures (Kopf Instruments, Tujunga, CA, USA).

Morris Water Maze (MWM) test: In the Morris water maze, the hidden platform procedure was performed in a circular tank filled with opaque water as described already with minor modifications (Vorhees and Williams, 2006; Mir et al., 2014; Sen and Sen, 2016). Both sham and TBI-mice received GSK2656157 for 24 days following TBI. After completion of treatments, mice underwent training for 6

days. Training period: For training, mice were placed in the tank at four random points and allowed to search and find the platform. In the event, the mouse didn't find the platform within the 60s time, the mouse was manually put on the platform for extra 30s. During the training, the mouse was allowed to search for the platform for the 60s. Two-trainings were given every day and the latency after two-trainings was recorded for each day for 6 days. Altogether 30 days (24 +6) were consumed for treatments and training.

Probe trial: After 24h of last training on day 30, a probe trial was performed on day 31 after TBI or sham. The mice were allowed to swim in the tank for the 60s without the platform, and performance was assessed on the basis of the time spent in the quadrant in which the hidden platform was originally located (the right quadrant).The mouse speed, time for thigmotaxis and time in each quadrant were analyzed using the data generated by the Any-maze software.

Neurite outgrowth: The dendritic length assay was performed as described (Sen and Snyder, 2011), with modifications. Briefly, primary neurons were transfected with GFP, and images of neuronal morphologies were captured based on immunoreactivities against GFP, using the 510 META confocal laser-scanning microscope (LSM) system (Zeiss, LA, USA) after treatment with either GSK2656157 (5mg/ml) or GSK2656157 (200 µg/ml) + tunicamycin (3 µg/ml). Dendrites and axons were identified by standard morphological criteria. Because the majority of neurons in our cortical culture preparation possessed only one clearly classifiable axon and one or more dendrites, neurons with non-pyramidal morphological features (such as multiple axons or no classifiable processes) were excluded from analyses. The total length was determined manually using Neuron J1.0.0 plug-in software for ImageJ (National Institutes of Health). Representative images were acquired using the 510 META confocal LSM with a 40× objective. All analyses were performed by an observer blinded to the identity of the transfected constructs.

Cortical Primary Neuronal culture and treatment: The preparation of the primary cortical neurons from wild-type mice was performed as described previously (Sen et al., 2008; Sen et al., 2009; Sen et al., 2012; Mir et al., 2014). The pregnant mice at the E18.5 of the gestational age based on the vaginal plug determination method were anesthetized with xylazine (8 mg/kg)/ketamine (60 mg/kg) and cleaned using 70% ethanol. The uterus was opened and pups were placed in sterile pre-chilled HBSS. Each pup was mounted on the stereomicroscope and cortices were dissected out. After enzyme based digestion, cortical neurons were counted and plated on the sterilized cover glass or 6-well plates in serum-free Neurobasal Medium supplemented with appropriate growth supplements (B27 and N2, Life Technologies). The medium was changed very 3-4 days. For the biochemical purposes, neurons were washed and scraped off and collected in lysis buffer with protease inhibitors. The protein content was estimated by Bradford

method. Primary neurons were treated with either tunicamycin (3µg/ml) and/or GSK2656157 (200µg/ml) for 24h in subsequent experiments. All experiments were performed with 10- to 12-day old cultures, at which time the cultures contain ~95–98% neurons and 2–5% astrocytes.

Transfection experiments were performed using the NeuroPORTER transfection kit (Sigma) following previously published protocol with modifications (Di Giovanni et al., 2005; Uchida et al., 2006; Chi and Nicol, 2007; Andres et al., 2011). The cells were rinsed once with Optimem media and incubated at 37°C for about 30 min. The Neuroporter–DNA complex (100 nM) was added on day 3 in a culture wherein the neurons were exposed to either Myc-PERK or Myc-PERK-K618A construct or Neuroporter alone for 48 h at 37°C. After 2 days (day 5 in culture), the Neuroporter ± DNA constructs were washed out and the normal media containing antibiotics and NGF was then added to the neurons and allowed to incubate for another 2 days before Western blots were performed.

Overexpression of constructs in mouse brain: Plasmid/polyethyleneimine (PEI) complexes including either PERK or PERK-K618A were injected into the cortex as published before (Jouvert et al., 2004; Wu et al., 2004; Schaffer et al., 2010; Uchida et al., 2010). A vector containing either Myc-PERK or Myc-PERK-K618A (obtained from Addgene, 7.5 µg) were complexed with 15 nmol of linear 22 kDa PEI in 5% glucose solution. Mixtures were allowed to equilibrate for 15 min at room temperature and were injected (0.5 µg per injection) into the cortex prior to TBI. 3.5µl of PEI–plasmid complexes were injected using a 10µl Hamilton syringe. After a wait of 5 min, the needle was slowly withdrawn.

Western blot and Co-immunoprecipitation: Whole tissue lysates were prepared from 3-mm coronal sections centered upon the site of impact. A 1-mm micro-punch was collected from the pericontusional cortex or from the corresponding pericontusional hemisphere as described previously (Farook et al., 2013; Kapoor et al., 2013; Mir et al., 2014; Sen and Sen, 2016). Tissue was placed in complete RIPA buffer, sonicated, and centrifuged for 120 min at 124 000 × g at 4 °C. Thirty micrograms of protein were resolved on a 4–20% SDS-polyacrylamide gel and transferred onto a polyvinylidene difluoride membrane. Blots were incubated overnight at 4 °C in primary antibody phosphorylated-PERK (Thr980; Cell Signaling), phosphorylated - PSD95 (T19; Abcam), phosphorylated-CREB (S129; Abcam), phosphorylated-eIF2α (S51; Abcam), PSD95 (Abcam), CREB (Cell Signaling), CBP (Santa Cruz), Actin (cell Signaling) and BDNF (Cell Signaling) followed by a 2 h incubation with an Alexa Fluor-tagged secondary antibody at room temperature, per our laboratory. Blots were visualized using a Li-Cor Odyssey near-infrared imaging system and densitometry analysis was performed using Quantity One software (Bio-Rad, Foster City, CA, USA) (Farook et al., 2013; Kapoor et al., 2013; Mir et al., 2014). The intensity of each band

was determined by Image J software and the changes in the experimental band was represented as fold changes as described previously (Sen et al., 2012) (Sen et al., 2008).

Protein-protein interactions were measured by co-immunoprecipitation assay per our method (Sen et al., 2008; Farook et al., 2013; Sen and Sen, 2016). Briefly, treated or untreated cells were lysed in lysis buffer [50 mM Tris (pH 7.4), 150 mM NaCl, 0.1% CHAPS, 100 µM deferoxamine and 1 mM EDTA) and homogenized by passage through a 26-gauge needle. Crude lysates were cleared of insoluble debris by centrifugation at 14,000 × g. Immunoprecipitation buffer [50mM Tris (pH 7.4), 150 mM NaCl, 0.1% CHAPS, 100 µM deferoxamine, 1 mM EDTA, and 0.1 mg/ml BSA] was added to 100 µg of cell lysates to bring samples to a total volume of 1000 µl. Cell lysates were incubated with either anti-CREB/CREB (S129) or anti-IgG antibody and 30µl of protein G agarose were added and incubated on a rotator at 4°C. The protein G agarose was washed four times with lysis buffer and quenched with 30 µl of SDS sample buffer. Co-immunoprecipitates were resolved by SDS-PAGE and analyzed by Western blotting either with anti-CBP antibodies.

Immunohistochemistry: Deeply anesthetized mice were perfused with saline, followed by fixation with 4% paraformaldehyde in 0.1 M phosphate buffer (pH 7.4). Brains were post-fixed overnight in paraformaldehyde followed by cryoprotection with 30% sucrose (pH 7.4) until brains permeated. Serial coronal sections were prepared using a cryostat microtome (Leica, Wetzlar, Germany) and directly mounted onto glass slides. Sections were incubated at room temperature with 100% normal donkey serum in phosphate-buffered saline containing 0.4% Triton X-100 for 12 h, followed by incubation with the primary antibody against phosphor-PERK(Thr980), phospsho-CREB (S129), phosphor-PSD95 (T19), Myc-PERK and Myc-PERK-K618A overnight at 4 °C. Sections were then washed and incubated with the appropriate Alexa Fluor-tagged secondary antibody. The omission of primary antibody served as a negative control (Sen and Snyder, 2011; Farook et al., 2013; Kapoor et al., 2013; Mir et al., 2014; Sen and Sen, 2016).

Confocal microscopy: Immunofluorescence was determined using an LSM 710 Meta confocal laser microscope (Carl Zeiss, Thornwood, NY, USA), as described previously. Cellular co-localization was determined in a Z-stack mode using 63X oil immersion Neofluor objective (NA 12.3) with the image size set at 512 × 512 pixels. The following excitation lasers/emission filters settings were used for various chromophores: argon2 laser was used for Alexa Fluor 488, with excitation maxima at 490 nm and emission in the range 505–530 nm. A HeNe1 laser was used for Alexa Fluor 594 with excitation maxima at 543 nm and emission in the range 568–615 nm. Z-stacks (20 optical slices) were collected at optimal

pinhole diameter at 12-bit pixel depth and converted into three-dimensional projection images using LSM 510 Meta imaging software (Carl Zeiss) (Sen et al., 2012; Kapoor et al., 2013; Sen and Sen, 2016).

DiI Stain and spine evaluation: Mice were deeply anesthetized with isoflurane and perfused transcardially with 0.9% saline solution. The brains were removed and stained using the Dil method as previously described (Stranahan et al., 2007; Erion et al., 2014). Coronal sections of 200 µm thickness from the cortex were obtained using a vibratome. These sections were collected on positive fixed microscope slides and dehydrated spontaneously. Spines were counted after image acquisition on secondary and tertiary branches of dendrites of neurons with or without treatment with GSK2656157 following either sham or TBI. Spine number was measured by Image J and analyzed by investigators who were blind to protocol. For analysis of dendritic spine morphology, image stacks were filtered and analyzed using Zeiss LSM 710 software. First, spines were identified based on the presence of a clearly resolved head and neck. For analysis of spine length, the full extent of the tracing was determined manually, from the point of contact with the dendritic shaft to the tip of the spine head.

In-vitro kinase assay: Recombinant PERK protein (2µg; Thermo Fisher Scientific) was incubated with either recombinant CREB (1.2µg; Novus Biologicals) or recombinant PSD95 protein (1.2µg; Novus Biologicals) in a kinase buffer (CST; 25 mM Tris-HCl (pH 7.5), 5 mM b-glycerophosphate, 2mM dithiothreitol (DTT), 0.1 mM Na3VO4, 10 mM MgCl2) supplemented with ATP (200 µM) at 37^0C for an hour. Then 40µl of the total reaction mixture was run on an SDS-PAGE gel. The phosphorylation level of CREB (S129) and PSD95 (S9) was monitored by Western blot hybridization using specific antibodies as mentioned above.

Experimental design and Statistical analysis: All data are presented as the mean ± SEM. The effects of treatments were analyzed using a one-way analysis of variance (ANOVA) followed by Dunnett's post hoc test. Results are expressed as mean ± S.E.M; n=5-7. A p-value <0.05 was considered to be statistically significant. Two-way repeated-measures ANOVAs with LSD posthoc tests were used to determine statistical significance between TBI and TBI+GSK2656157 groups for all training days during MWM tests; n=7. One-way ANOVAs with the appropriate LSD posthoc tests were used to compare experimental groups. For all analyses, $p < 0.05$ was considered significant. We use C57BL/6 male mice through out our experiments.

Results

Treatment with GSK2656157 prevents PERK phosphorylation but not phosphorylation of eIF2α following TBI

PERK is an ER-kinase and upon induction of either unfolded protein response or ER-stress PERK is activated by increasing its phosphorylation status (Harding et al., 2000; Zhang et al., 2002; Wek and Cavener, 2007; Saito et al., 2011). Activated PERK phosphorylates eIF2α, which is known to inhibit protein synthesis. To see whether TBI has any influence on phosphorylation of PERK and/or eIF2α, we measured their levels in the pericontusional cortex. We found that TBI leads to an increase in the phosphorylation level of both PERK (Thr980) and eIF2α (S51) to about 3.5 and 2.6 fold respectively (Fig. 2A). We have also tested the activation of ATF6 and IRE1α following TBI. We found that the cleaved level of ATF6 was not increased following TBI, which suggests that ATF6 pathway has not been activated following TBI (Fig. 2B). IRE1α is a Ser/Thr protein kinase that possesses endonuclease activity. ER-stress can activate IRE1 α by inducing its phosphorylation level. We found that the phosphorylation level of IRE1α has not altered following TBI (Fig. 2C). This data suggests that TBI does not induce the activation of IRE1α in our experimental condition of TBI.

We were interested to see whether treatment with an inhibitor of PERK phosphorylation, GSK2656157 has any influence on phosphorylation of both PERK and eIF2α. We treated wild-type mice with GSK2656157 in a dose-dependent manner (10-50 mg/kg) following TBI and phosphorylation of PERK and eIF2α was measured through Western blot analysis in the pericontusional cortex. Interestingly, we found that treatment with GSK2656157 causes a decrease in PERK phosphorylation in a dose-dependent manner, however, the phosphorylation level of eIF2α remains unaltered throughout the treatment (Fig. 2F). We also found that treatment with 50 mg/kg of GK2656157 is enough to fully block the induction of phosphorylation of PERK following TBI (Fig. 2D), however, the phosphorylation level of eIF2α remains unaltered. Consistent with treatment with GSK2656157, we found that overexpression of the kinase-dead construct of PERK does not reduce phosphorylation level of eIF2α (Fig. 2E). To further confirm the alteration of PERK phosphorylation after GSK2656157 treatment, we performed confocal microscopy analysis. Consistent with our Western blot data, we found that treatment with GSK2656157 (50 mg/kg) reduces PERK phosphorylation significantly (Fig. 2F).

In another set of experiments, primary neurons were treated with an ER-stress inducer, tunicamycin in the presence or absence of GSK2656157. We found that treatment with tunicamycin causes an increase in both PERK and eIF2α phosphorylation level; however, the induction of PERK phosphorylation was abolished in the presence of GSK2656157, but the phosphorylation level of eIF2α remains unaltered (Fig. 2G).

Treatment with GSK2656157 restores spine density and memory deficits following TBI

Since treatment with GSK2656157 was shown to prevent PERK phosphorylation independent of eIF2α phosphorylation in pericontusional cortex following TBI, we were interested to see whether it has any effect on spine density and performance in memory functions. Dendritic spines were visualized in slices from GSK2656157- and vehicle-treated wild-type mice using the lipophilic membrane tracer DiI. After Dil staining, TBI mice have fewer dendritic spines than wildtype mice. Moreover, GSK2656157 treatment normalizes dendritic spine density (Fig. 3A, B) along the spine length (Fig. 3A, C) and spine surface area (Fig. 3A, D) following TBI.

To monitor whether treatment with GSK2656157 has any influence on memory impairment following TBI, both TBI and TBI + GSK2656157 group of mice along with sham mice were subjected to Morris water maze tests after TBI. We found that on the first day of training, the latency to find the platform for either sham or sham + GSK2656157 treated mice starts from around 30s, however, after 6 days of training they can reach the platform around 15s (Fig. 3E). Compared to sham mice, TBI mice did not improve their memory functions even after 6 days of training. In contrast, treatment with GSK2656157, TBI mice gradually performed better than TBI mice. The latency for TBI + GSK2656157 on the first day was close to 58s (vs TBI 60s). After 6 days of training the latency to find the platform for TBI+GSK2656157 treated mice was around 45s (vs TBI 58s) (Fig. 3E). Interestingly, two-way ANOVA analysis between the TBI and TBI+GSK2656157 treated groups for different time points shows that data are significant only at 2,5 and 6 days following TBI. On the day of probe trial the trend for the latency to find the platform remains unaltered (Fig. 3F). To further confirm how the treatment with GSK2656157 affects their memory function, we have monitored the percentage (%) of time spent in each quadrant.

We found that either sham or sham + GSK2656157 treated mice spent around 70% of the time in the quadrant where the platform was located (TQ; target quadrant) compared to TBI-mice which have spent around 30% time in the 'TQ' quadrant. Interestingly, treatment with GSK2656157 following TBI rescues the percentage of time in the 'TQ' quadrant (Fig. 3G). Here we have also measured mouse speed for sham, sham+GSK2656157, TBI and TBI+GSK2656157 treated mice. We did not observe any significant difference in mouse speed irrespective of their groups (Fig. 3H). This data suggests that MWM learning impairments are independent of locomotor effects because land-based locomotor reductions did not affect swimming speed. Another important aspect of MWM tests is thigmotaxis, or the tendency to cling or follow the wall around the outer perimeter of the tank, which serves as one index to reflect that the animal is not problem-solving. On the day of probe trial, the percentage of time for thigmotaxis in either sham or sham + GSK2656157 is not more than 5-7%; however, the % of the time for thigmotaxis

of TBI mice is around 20%. Interestingly, treatment with GSK2656157 has reduced the % of the time for thigmotaxis of TBI mice (Fig. 3I). Taken together, our data suggests that treatment with GSK2656157 improves the learning and memory functions following TBI.

Active PERK inactivates CREB via phosphorylation at S129 following TBI

CREB is a transcription factor which is known to transcribes several genes including BDNF that regulate formation and maintenance of memory (Finkbeiner et al., 1997; Tao et al., 1998; Herold et al., 2011). To see whether activation of PERK has any influence on CREB phosphorylation, we monitor its level via Western Blot hybridization. We found that phosphorylation level of CREB at serine 129 (S129) was increased significantly, however, the phosphorylation level at serine 133 (S133) remains unaltered following TBI (Fig. 4A). To further confirm the alteration of CREB phosphorylation, we performed confocal microscopy analysis where phosphorylation CREB at S129 was monitored by green fluorescence intensity. We found that TBI leads to an increase in CREB phosphorylation at S129 residue which was indicated by an increase in green fluorescent intensity (Fig. 4B). Since activation of CREB depends on its interaction with a coactivator, CBP protein, we monitor the interaction between CREB and CBP by co-immunoprecipitation assay. We found that the interaction between CREB and CBP and phosphorylated CREB at S129 residue and CBP was decreased significantly (Fig. 4C) along with a decrease in BDNF protein level (Fig. 4D) in pericontusional cortex following TBI.

To see whether treatment with GSK2656157 can prevent CREB phosphorylation at S129 and BDNF level, mice were treated with GSK2656157 following TBI and phosphorylation level of CREB was monitored by Western blot hybridization assay. We found that the increase CREB phosphorylation at S129 was decreased significantly in mice treated with GSK2656157 following TBI (Fig. 3E). Similarly, the protein level of BDNF was restored in TBI+GSK2656157 treated mice compared to TBI mice (Fig. 4E). To further confirm whether the alteration of CREB phosphorylation is directly regulated by activation of PERK following TBI, we overexpressed kinase-dead mutant of PERK (PERK-K618A) through injection in cortex prior to TBI. Consistent with the data resulted from the treatment of GSK2656157, we found that overexpression of PERK-K618A prevents the induction of CREB phosphorylation at S129 residue and rescues the protein level of BDNF compared to mice overexpressed with lentiviral particles of control vector construct (Fig. 4F). This data suggests that an increase in phosphorylation of CREB at S129 compromises its interaction with CBP and subsequent transcriptional activity and BDNF level following TBI. The loss of BDNF can be restored by preventing activation of PERK via preventing CREB's phosphorylation at S129 residue.

Previously, it was reported that activation of GSK3β can directly phosphorylate CREB at S129 residue (Bullock and Habener, 1998; Grimes and Jope, 2001) and TBI can activate GSK3β by reducing the activation of a protein kinase, Akt (Farook et al., 2013). To test whether induction of CREB phosphorylation at S129 can be blocked by a GSK3β inhibitor, lithium, we treated TBI-mice with lithium in the presence or absence of GSK2656157. We found that treatment with lithium has no effect on CREB phosphorylation at S129; however, GSK2656157 can block CREB phosphorylation at S129 irrespective of the treatment with lithium (Fig. 4G). Administration of lithium can block the activation of GSK3β by increasing the level of phosphorylation of GSK3β following TBI. Taken together, this data suggests that activated PERK can phosphorylate CREB at S129.

To further confirm whether PERK can directly phosphorylate CREB, we incubated recombinant PERK protein along with recombinant CREB protein in the kinase buffer in the presence or absence of ATP. The reaction mixtures ran into the SDS-PAGE gel and phosphorylation of CREB was detected by Western blot hybridization. We found that CREB phosphorylation at S129 was detected only in the sample which contains ATP (Fig. 4H).

Since CREB's transcriptional activity and BDNF were decreased due to an increase in PERK phosphorylation, we were interested to see whether inhibition of PERK has any effect on dendritic length. Primary neurons were treated with GSK2656157 prior to exposure of cells to an ER-stress inducer, tunicamycin. We found that the total dendritic length was decreased significantly after exposure to tunicamycin, however, treatment with GSK2656157 can rescue the loss of total dendritic length in primary neurons exposed to tunicamycin (Fig. 4I). Our data was further confirmed by overexpression of a kinase-dead mutant of PERK in primary neurons before treatment with tunicamycin. We found that tunicamycin results in the loss of total dendritic length, however, cells overexpressed with a kinase-dead mutant of PERK (PERK-K618A) rescues the loss of total dendritic length following treatment with tunicamycin (Fig. 4J).

Phosphorylation of PSD95 at T19 by activated PERK causes its downregulation following TBI

PSD95 is a scaffold protein and is known to promote synapse maturation and exerts a major influence on synaptic stability, memory formation in the brain (El-Husseini et al., 2000; Beique and Andrade, 2003; Kim and Sheng, 2004; Ehrlich et al., 2007). To see whether TBI has any influence on phosphorylation of PSD95, we monitored the phosphorylation level of PSD95 by Western blot hybridization. We found that TBI leads to an increase in phosphorylation of PSD95 at T19 residue (Fig.

5A). It was further confirmed by confocal microscopy where phosphorylation of PSD95 was monitored by green fluorescence intensity (Fig. 5B).

To monitor, whether treatment with GSK2656157 has any influence on phosphorylation of PSD95 at T19 residue, we treated mice with GSK2656157 after TBI. Interestingly we found that treatment with GSK2656157 markedly reduces the increase in TBI-induced augmentation of PSD95 phosphorylation at T19 residue (Fig. 5C). To see whether inhibition of PERK phosphorylation directly affects phosphorylation of PSD95, we overexpressed a kinase-dead mutant of PERK (PERK-K618A) into the cortex prior to TBI. we found that mice overexpressed with PERK-K618A prevent the increase in PSD95 phosphorylation at T19 residue compared to mice overexpressed with the control vector (Fig. 5D). Previously it was shown that phosphorylation of PSD95 at T19 residue affects its stability (Nelson et al., 2013). We were interested to see whether inhibition of PERK phosphorylation influences the protein level of PSD95 following TBI. We found that TBI leads to a decrease in PSD95 protein level significantly (Fig. 5D). However, overexpression of PERK-K618A rescues the loss of PSD95 protein level along with a decrease in phosphorylation of PSD95 at T19 residue (Fig. 5D). This data suggests that TBI-induced decrease in PSD95 is dependent on its phosphorylation status at T19 residue, but this can be rescued by preventing PERK phosphorylation in mice following TBI.

Activation of GSK3β is known to phosphorylate PSD95 at T19. Considering the fact that TBI leads to an activation of GSK3β, we were interested to see whether blocking GSK3β activation can rescue PSD95 phosphorylation at T19 residue. TBI-mice were treated with a GSK3β inhibitor, lithium along with the administration of a PERK-kinase inhibitor, GSK2656157. We found that treatment with lithium has no effect on PSD95 phosphorylation; however preventing PERK phosphorylation by GSK2656157 significantly reduces PSD95 phosphorylation at T19 residue independent of the treatment with lithium (Fig. 5E). Administration of lithium can block the activation of GSK3β by increasing the level of phosphorylation of GSK3β following TBI. Taken together, this data suggests that activation of PERK is directly responsible for PSD95 phosphorylation at T19 residue.

To further confirm whether PERK can directly phosphorylate PSD95, we incubated a recombinant PERK protein along with recombinant PSD95 protein in the kinase buffer in the presence or absence of ATP. The reaction mixtures ran into the SDS-PAGE gel and phosphorylation of PSD95 was monitored by Western lot hybridization using an antibody specific to phospho-PSD95 at T19 residue. We found that PSD95 phosphorylation at T19 was detected only in the sample which contains ATP (Fig. 5F). The phosphorylated and unphosphorylated level of PSD95 was also detected by PSD95 antibody. This data validates the reliability of the antibody specific for phosphorylation of PSD95.

To see whether activation of PERK has any influence on PSD95 positive puncta numbers, we treated primary neurons with GSK2656157 prior to exposure with ER-stress activator, tunicamycin. We found that exposure of tunicamycin causes a significant decrease in PSD95 positive puncta number (Fig. 4G,H) and size of PSD95 positive puncta (Fig. 5G, I), however, in cells treated with GSK2656157 prior to tunicamycin prevents the loss of PSD95 positive puncta number (Fig. 5G,H) and the size of PSD95 positive puncta (Fig. 5G, I) along with a decrease in phosphorylation of PSD95 at T19 residue in cells treated with tunicamycin. Consistent with this data, overexpression of PERK-K618A in primary neurons rescues tunicamycin-induced loss of PSD95 positive puncta number (Fig. 5J,K) and the size of PSD95 positive puncta (Fig. 5J, L). Taken together, these results suggest that activation of PERK directly affects PSD95 level by increasing its phosphorylation level.

Discussion:

In the present study, we have demonstrated a novel mechanism whereby activation of PERK causes an impairment of memory through inactivation of CREB protein and downregulation of PSD95. An increased level of phosphorylation of CREB at S129 prevents its transcriptional activity and phosphorylation of PSD95 at T19 leads to its downregulation following TBI (Fig. 5M). We have also shown that inhibiting phosphorylation of PERK by using GSK2656157 restores memory deficiency and neurite outgrowth by reducing phosphorylation of CREB and PSD95, but without affecting the elevated level of phosphorylation of an initiation factor eIF2α.

PERK is a ubiquitous ER-localized protein kinase and global inactivation of PERK in mice results in multiple developmental defects, including early onset diabetes, growth retardation, skeletal abnormalities, and pancreatic atrophy (Harding et al., 2001; Zhang et al., 2002). In the brain, PERK functions in the cortex as a physiological constraint of memory consolidation, and its downregulation serves as a cognitive enhancement by phosphorylating eIF2α at S51 residue. In wild-type mice, brain-specific deletion of PERK protein has been shown to impair cognitive functions and behavioral flexibility (Trinh et al., 2012) and this data is consistent with studies where either GCN2 KO mice (Costa-Mattioli et al., 2005) or eIF2α-S51A mutant mice (Costa-Mattioli et al., 2007) have shown facilitation of memory. In TBI, treatment with either salubrinal (Rubovitch et al., 2015) or docosahexaenoic acid (Begum et al., 2014; Desai et al., 2014) has been shown to prevent phosphorylation of eIF2α and acts as a neuroprotective agent. Consistent with TBI data, elevated phosphorylation of eIF2α has been observed in the brains of Alzheimer's disease (AD) patients and AD model mice (Chang et al., 2002; O'Connor et al., 2008; Ma et al., 2013). Genetic deletion of PERK prevented enhanced phosphorylation of eIF2α and

deficits in protein synthesis, synaptic plasticity and spatial memory in mice that express familial AD-related mutations in APP and PSEN1.

In this manuscript, we have shown that inhibition of PERK phosphorylation does not affect phosphorylation of eIF2a but rescues the deficiency of synaptic plasticity significantly. This data suggests that PERK phosphorylation may function independently of the phosphorylation of eIF2a but it is not exclusively independent of eIF2a. Other literature suggest that An aberrant eIF2α phosphorylation was associated with synaptic pathophysiology and memory dysfunction following AD (Ma et al., 2013). Moreover, UPR-mediated translational failure was shown as a generic pathogenic mechanism in protein-misfolding disorders, including tauopathies (Radford et al., 2015). Taken together it suggests that phosphorylation of PERK and eIF2α both contributes to the deterioration of synaptic plasticity but their individual contribution varies from context to context. Recent studies suggest that treatment with the small molecule ISRIB, which restores translation downstream of eIF2α, conferred neuroprotection in prion-diseased mice without adverse effects on the pancreas (Halliday et al., 2015). We have used GSK2656157 as a PERK phosphorylation inhibitor to study its role in deficiencies in synaptic plasticity following TBI. We anticipate that treatment with ISRIB will lead to PSD95 reduction and CREB-related dysfunction.

In addition, our data is consistent with the previous finding where it was shown that treatment with GSK2656157 inhibits PERK activity in the mouse pancreas (Atkins et al., 2013) but did not inhibit downstream PERK signalings such as phospho-eIF2α, ATF, or CHOP protein levels. This data suggests that inhibition of PERK activity by GSK2656157 does not always correlate with inhibition of eIF2α phosphorylation or mimic the biological effects of genetic inactivation of PERK. Moreover, the initiation factor, eIF2α can be phosphorylated by several kinases such GCN2, PKR, and HRI other than PERK (Ohno, 2014). Thus, it is possible that preventing phosphorylation of PERK does not necessarily block phosphorylation of eIF2α. At the same time, our data indicates that the phosphorylation of eIF2α could be dispensable to restore memory deficits following TBI.

Multiple studies have shown that significant loss of synapses in the days after brain injury (Gao and Chen, 2011; Gao et al., 2011; Park and Biederer, 2013) are responsible for memory deficits following TBI. Dendritic spines are the postsynaptic protrusions through which neurons receive most of their excitatory input. Gao et al. showed in a mouse model that after TBI, there are fewer dendritic synaptic spines in the cortex and hippocampus (Gao and Chen, 2011; Gao et al., 2011). The formation of synapses and spine density depends on the level of postsynaptic scaffold protein PSD95 and BDNF level which can be transcribed by CREB.

The activation of CREB depends on its phosphorylation level. Compelling numbers of evidence have suggested that phosphorylation of CREB at S133 is essential for its transcription; however phosphorylation of CREB at S129 has reached two opposite conclusions. Fiol et al. reported that GSK3β facilitated activation of CREB by increasing its phosphorylation status (Fiol et al., 1994). In contrast, Bullock and Habener found that phosphorylation of CREB by GSK3β attenuated DNA binding activity of CREB (Bullock and Habener, 1998). This study was further supported by Grimes et al where it was shown that GSK3β negatively regulates CREB DNA binding activity and that lithium and sodium valproate, inhibitors of GSK3β, facilitate CREB activation (Grimes and Jope, 2001). Consistent with these studies, we found that PERK directly phosphorylates CREB at S129 residue without altering its phosphorylation status at S133. To further elucidate the underlying mechanism, we have shown that phosphorylation of CREB at S129 prevents its interaction with a coactivator CBP that leads to its transcriptional inactivation and downregulation of BDNF. On the other hand, PSD95, a major scaffold protein of the postsynaptic density (PSD) that promotes synaptic strength can be phosphorylated by GSk3β at T19 residue (Nelson et al., 2013). Phosphorylation of PSD95 affects the stability in dendritic spines that can be reversed by overexpression of T19A mutant of PSD95.

However, the question arises whether activation of GSK3β can also contribute to the phosphorylation of both CREB and PSD95 proteins following TBI, particularly considering the fact that TBI leads to an activation of GSK3β by reducing its phosphorylation at S9 residue (Farook et al., 2013). Here we have shown that inhibition of GSK3β by using lithium cannot prevent the phosphorylation of either CREB or PSD95 in the pericontusional cortex; however, inhibition of PERK phosphorylation abolish the phosphorylation level of CREB and PSD95 following TBI. This data suggests that activation of PERK is directly responsible for phosphorylation of CREB and PSD95 following TBI which was further supported by *in-vitro* phosphorylation assay. Moreover, treatment with PERK inhibitor blocks CREB and PSD95 phosphorylation without having any effect on eIF2α phosphorylation. This data suggests that eIF2α is not responsible for phosphorylation of CREB and PSD95 following TBI. We have also shown that inhibition of PERK activation restores dendritic spines, spine length and spine surface area along with a decrease in PSD95 and CREB phosphorylation at T19 and S129 residues respectively following TBI. To our knowledge, our study may provide the first evidence that CREB and PSD95 can be directly phosphorylated by PERK following TBI.

Collectively, these results provide a novel mechanism where PERK-phosphorylation impairs memory by inactivating CREB and downregulation of PSD95 following TBI. Inhibiting PERK-phosphorylation rescues spine density and dendritic outgrowth following TBI. Thus, our study provides a

framework on which PERK-phosphorylation inhibitor such as GSK2656157 can be tested as a therapeutic approach to prevent memory impairment in TBI patients.

Figure Legends:

Figure 1: **Experimental design for TBI mice after with or without treatment with GSK2656157. (A-B)**, mice were treated with GSK2656157 for 24 days following TBI. Then biochemical analysis was done on the 25th day. In other experiments, the mice were trained for MWM test for 6 days after completion of GSK2656157 treatment of TBI mice and the probe trial was done on the 31st day of TBI. The same sets of mice were used to monitor the synaptic density of TBI or sham mice on the 31st day following TBI. **(C)** either PERK or PERK-K618A was overexpressed in mice brain 7 days before TBI. Then biochemical analysis was performed on the 25th day after TBI. The procedure for TBI and overexpression of PERK/PERK-K618A were described in the following sections.

Figure 2: **Treatment with GSK2656157 reduces PERK phosphorylation. (A)** Western blot analysis of the expression of PERK and eIF2α phosphorylation in pericontusional cortex following TBI. *p<0.05, n=9, one-way ANOVA, mean ± Standard Error Mean. **(B)** Western blot analysis to measure uncleaved and cleaved ATF6 following sham or TBI. **(C)** Western blot analysis to measure phosphorylation level of IRE1α following TBI. **(D)** Western Blot analysis of phosphorylation of both PERK and eIF2α after treatment with GSK2656157 at 10 mg/kg, 20 mg/kg, and 50 mg/kg following TBI. *p<0.05, n=5, one-way ANOVA, mean ± Standard Error Mean. **(E)** Western blot analysis of eIF2α phosphorylation after overexpression of either PERK or PERK-K618A in mouse brain prior to TBI. The overexpression of PERK was monitored by Western blot hybridization. **(F)** Confocal microscopic analysis to measure PERK phosphorylation with or without GSK2656157 treatment following TBI. **(G)** Primary neurons were treated with tunicamycin (3μg/ml) with or without GSK2656157 (15μg/ml) treatment for 6h and phosphorylation of PERK and eIF2α were monitored by Western blot hybridization. *p<0.05, n=9, one-way ANOVA, mean ± Standard Error Mean.

Figure 3: **Effect of GSK2656157 on spine density and memory functions following TBI. (A-D)** Dendritic spines /10μm **(A-B)**, spine length **(A, C)** and spine surface area **(A, D)** were measured after treatment with GSK2656157 (50 mg/kg) following TBI. *p<0.05, n=5, one-way ANOVA, mean ± Standard Error Mean. **(E-F)** The latency to find the platform during training period of 6 days (at the end of two trials in a day (**E**) *p<0.05, n=7, two-way ANOVA between TBI and TBI+GSK2656157 groups for all days during training; mean ± Standard Error Mean; and the day of probe trial (**F**) (**G**) The percentage of time in each quadrant was measured for Sham, Sham + GSK2656157, TBI and

TBI+GSK2656157 treated groups. The quadrant which has the platform was designated as 'TQ; target quadrant' and the quadrant from where the mice started their swimming was designated as 'OP; opposite'. The quadrant on the left side of 'OP' was designated as 'AL: adjacent left' and the quadrant on the right side of 'OP' quadrant was designated as 'AR; adjacent right'. *p<0.05, n=5-6, two-way ANOVA, mean ± Standard Error Mean (H) Mouse speed was monitored in Sham, Sham + GSK2656157, TBI and TBI+GSK2656157 treated groups. (I) the percentage of time for thigmotaxis was monitored in Sham, Sham + GSK2656157, TBI and TBI+GSK2656157 treated groups. *p<0.05, n=10-12, one-way ANOVA, mean ± Standard Error Mean.

Figure 4: **Effect of GSK2656157 on CREB phosphorylation and dendritic outgrowth**. **(A)** Western blot analysis of CREB phosphorylation at S129 and S133 in pericontusional cortex after TBI. *p<0.05, n=5, one-way ANOVA, mean ± Standard Error Mean. **(B)** Confocal microscopic analysis of CREB phosphorylation (S129). **(C)** Co-immunoprecipitation assay to monitor the interaction between either CREB or phospho-CREB (S129) and CBP after TBI. **(D)** Western blot analysis of BDNF protein level. **(E)** Western blot analysis of the protein level of CREB phosphorylation (S129) and BDNF following GSK2656157 treatment after TBI. **(F)** Confocal microscopic analysis of Myc in cortex after overexpression of either Myc-PERK or Myc-PERK-K618A. Western blot analysis to monitor CREB phosphorylation at S129, BDNF, Actin, and Myc protein levels after TBI. *p<0.05, n=8-10, one-way ANOVA, mean ± Standard Error Mean. **(G)** Western blot analysis to monitor CREB phosphorylation at S129 after treatment with lithium (5mg/kg) with or without the addition of GSK2656157. *p<0.05, n=5, one-way ANOVA, mean ± Standard Error Mean. (**H**) In vitro kinase assay for CREB phosphorylation by PERK. Western blot analysis to monitor CREB phosphorylation at S129 residue. **(I-J)** Primary neurons were overexpressed with GFP and treated with isoflurane. Neurons were imaged by confocal microscopy to monitor dendritic morphology. **(I)** The total dendritic length was measured after GSK2656157 treatment and **(J)** cells overexpressed with either PERK or PERK-K618A before treatment with tunicamycin. *p<0.05, n=8-10, one-way ANOVA, mean ± Standard Error Mean.

Figure 5: **Effect of GSK2656157 on PSD95 phosphorylation and puncta numbers. (A)** Western blot analysis of PSD95 phosphorylation at T19 following TBI. *p<0.05, n=9, one-way ANOVA, mean ± Standard Error Mean. **(B)** Confocal microscopic analysis of PSD95 phosphorylation at T19 after TBI. **(C)** Western blot analysis of PSD95 phosphorylation (T19) after treatment with GSK2656157. *p<0.05, n=5, one-way ANOVA, mean ± Standard Error Mean. **(D)** Western blot analysis and quantitative measurement to monitor PSD95 phosphorylation and protein level of PSD95 after overexpression of either PERK wild type or PERK-K618A in the cortex. *p<0.05, n=5, one-way ANOVA, mean ± Standard Error Mean. **(E)** Western blot analysis to monitor PSD95 phosphorylation at T19 after treatment with lithium (1mM) with

565 or without the addition of GSK2656157. (**F**) In vitro kinase assay for PSD95 phosphorylation by PERK.
566 Western blot analysis to monitor PSD95 phosphorylation at T19 residue. **(G-I)** Confocal microscopic
567 analysis of the number (G, H) and size (G, I) of PSD95-positive puncta after tunicamycin treatment with
568 or without GSK2656157. *p<0.05, n=9, one-way ANOVA, mean ± Standard Error Mean. **(J-L)** Confocal
569 microscopic analysis of the number **(J, K)** and size (**J, L**) of PSD95-positive puncta in cells
570 overexpressed with either PERK or PERK-K618A mutant following TBI. *p<0.05, n=8-10, one-way
571 ANOVA, mean ± Standard Error Mean. **(M)** A schematic representation showing that TBI leads to an
572 increase in PERK phosphorylation which will subsequently phosphorylate CREB and PSD95 at S129 and
573 T19 residues respectively. The increase in CREB phosphorylation causes a downregulation of BDNF
574 level and PSD95 phosphorylation causes its downregulation after TBI. These events lead to spine loss and
575 memory impairment following TBI.

576

577 **References**

578 Andres RH, Choi R, Pendharkar AV, Gaeta X, Wang N, Nathan JK, Chua JY, Lee SW, Palmer TD, Steinberg
579 GK, Guzman R (2011) The CCR2/CCL2 interaction mediates the transendothelial recruitment of
580 intravascularly delivered neural stem cells to the ischemic brain. Stroke; a journal of cerebral
581 circulation 42:2923-2931.
582 Atkins C, Liu Q, Minthorn E, Zhang SY, Figueroa DJ, Moss K, Stanley TB, Sanders B, Goetz A, Gaul N,
583 Choudhry AE, Alsaid H, Jucker BM, Axten JM, Kumar R (2013) Characterization of a novel PERK
584 kinase inhibitor with antitumor and antiangiogenic activity. Cancer research 73:1993-2002.
585 Banhegyi G, Baumeister P, Benedetti A, Dong D, Fu Y, Lee AS, Li J, Mao C, Margittai E, Ni M, Paschen W,
586 Piccirella S, Senesi S, Sitia R, Wang M, Yang W (2007) Endoplasmic reticulum stress. Annals of
587 the New York Academy of Sciences 1113:58-71.
588 Begum G, Harvey L, Dixon CE, Sun D (2013) ER stress and effects of DHA as an ER stress inhibitor.
589 Translational stroke research 4:635-642.
590 Begum G, Yan HQ, Li L, Singh A, Dixon CE, Sun D (2014) Docosahexaenoic acid reduces ER stress and
591 abnormal protein accumulation and improves neuronal function following traumatic brain
592 injury. The Journal of neuroscience : the official journal of the Society for Neuroscience 34:3743-
593 3755.
594 Beique JC, Andrade R (2003) PSD-95 regulates synaptic transmission and plasticity in rat cerebral cortex.
595 The Journal of physiology 546:859-867.
596 Bonni A, Ginty DD, Dudek H, Greenberg ME (1995) Serine 133-phosphorylated CREB induces
597 transcription via a cooperative mechanism that may confer specificity to neurotrophin signals.
598 Molecular and cellular neurosciences 6:168-183.
599 Bullock BP, Habener JF (1998) Phosphorylation of the cAMP response element binding protein CREB by
600 cAMP-dependent protein kinase A and glycogen synthase kinase-3 alters DNA-binding affinity,
601 conformation, and increases net charge. Biochemistry 37:3795-3809.
602 Chang RC, Wong AK, Ng HK, Hugon J (2002) Phosphorylation of eukaryotic initiation factor-2alpha
603 (eIF2alpha) is associated with neuronal degeneration in Alzheimer's disease. Neuroreport
604 13:2429-2432.

Cheng D, Hoogenraad CC, Rush J, Ramm E, Schlager MA, Duong DM, Xu P, Wijayawardana SR, Hanfelt J, Nakagawa T, Sheng M, Peng J (2006) Relative and absolute quantification of postsynaptic density proteome isolated from rat forebrain and cerebellum. Molecular & cellular proteomics : MCP 5:1158-1170.

Chi XX, Nicol GD (2007) Manipulation of the potassium channel Kv1.1 and its effect on neuronal excitability in rat sensory neurons. Journal of neurophysiology 98:2683-2692.

Desai A, Kevala K, Kim HY (2014) Depletion of brain docosahexaenoic acid impairs recovery from traumatic brain injury. PloS one 9:e86472.

Di Giovanni S, De Biase A, Yakovlev A, Finn T, Beers J, Hoffman EP, Faden AI (2005) In vivo and in vitro characterization of novel neuronal plasticity factors identified following spinal cord injury. The Journal of biological chemistry 280:2084-2091.

Ehrlich I, Klein M, Rumpel S, Malinow R (2007) PSD-95 is required for activity-driven synapse stabilization. Proceedings of the National Academy of Sciences of the United States of America 104:4176-4181.

El-Husseini AE, Schnell E, Chetkovich DM, Nicoll RA, Bredt DS (2000) PSD-95 involvement in maturation of excitatory synapses. Science 290:1364-1368.

Erion JR, Wosiski-Kuhn M, Dey A, Hao S, Davis CL, Pollock NK, Stranahan AM (2014) Obesity elicits interleukin 1-mediated deficits in hippocampal synaptic plasticity. The Journal of neuroscience : the official journal of the Society for Neuroscience 34:2618-2631.

Farook JM, Shields J, Tawfik A, Markand S, Sen T, Smith SB, Brann D, Dhandapani KM, Sen N (2013) GADD34 induces cell death through inactivation of Akt following traumatic brain injury. Cell death & disease 4:e754.

Finkbeiner S, Tavazoie SF, Maloratsky A, Jacobs KM, Harris KM, Greenberg ME (1997) CREB: a major mediator of neuronal neurotrophin responses. Neuron 19:1031-1047.

Fiol CJ, Williams JS, Chou CH, Wang QM, Roach PJ, Andrisani OM (1994) A secondary phosphorylation of CREB341 at Ser129 is required for the cAMP-mediated control of gene expression. A role for glycogen synthase kinase-3 in the control of gene expression. The Journal of biological chemistry 269:32187-32193.

Gao X, Chen J (2011) Mild traumatic brain injury results in extensive neuronal degeneration in the cerebral cortex. Journal of neuropathology and experimental neurology 70:183-191.

Gao X, Deng P, Xu ZC, Chen J (2011) Moderate traumatic brain injury causes acute dendritic and synaptic degeneration in the hippocampal dentate gyrus. PloS one 6:e24566.

Ginty DD, Bonni A, Greenberg ME (1994) Nerve growth factor activates a Ras-dependent protein kinase that stimulates c-fos transcription via phosphorylation of CREB. Cell 77:713-725.

Grimes CA, Jope RS (2001) CREB DNA binding activity is inhibited by glycogen synthase kinase-3 beta and facilitated by lithium. Journal of neurochemistry 78:1219-1232.

Halliday M, Radford H, Sekine Y, Moreno J, Verity N, le Quesne J, Ortori CA, Barrett DA, Fromont C, Fischer PM, Harding HP, Ron D, Mallucci GR (2015) Partial restoration of protein synthesis rates by the small molecule ISRIB prevents neurodegeneration without pancreatic toxicity. Cell death & disease 6:e1672.

Harding HP, Zhang Y, Ron D (1999) Protein translation and folding are coupled by an endoplasmic-reticulum-resident kinase. Nature 397:271-274.

Harding HP, Zhang Y, Bertolotti A, Zeng H, Ron D (2000) Perk is essential for translational regulation and cell survival during the unfolded protein response. Molecular cell 5:897-904.

Harding HP, Zeng H, Zhang Y, Jungries R, Chung P, Plesken H, Sabatini DD, Ron D (2001) Diabetes mellitus and exocrine pancreatic dysfunction in perk-/- mice reveals a role for translational control in secretory cell survival. Molecular cell 7:1153-1163.

652 Herold S, Jagasia R, Merz K, Wassmer K, Lie DC (2011) CREB signalling regulates early survival, neuronal
653 gene expression and morphological development in adult subventricular zone neurogenesis.
654 Molecular and cellular neurosciences 46:79-88.
655 Jouvert P, Revel MO, Lazaris A, Aunis D, Langley K, Zwiller J (2004) Activation of the cGMP pathway in
656 dopaminergic structures reduces cocaine-induced EGR-1 expression and locomotor activity. The
657 Journal of neuroscience : the official journal of the Society for Neuroscience 24:10716-10725.
658 Kapoor S, Kim SM, Farook JM, Mir S, Saha R, Sen N (2013) Foxo3a transcriptionally upregulates AQP4
659 and induces cerebral edema following traumatic brain injury. The Journal of neuroscience : the
660 official journal of the Society for Neuroscience 33:17398-17403.
661 Kim E, Sheng M (2004) PDZ domain proteins of synapses. Nature reviews Neuroscience 5:771-781.
662 Krishnamoorthy J, Rajesh K, Mirzajani F, Kesoglidou P, Papadakis AI, Koromilas AE (2014) Evidence for
663 eIF2alpha phosphorylation-independent effects of GSK2656157, a novel catalytic inhibitor of
664 PERK with clinical implications. Cell cycle 13:801-806.
665 Larner SF, Hayes RL, Wang KK (2006) Unfolded protein response after neurotrauma. Journal of
666 neurotrauma 23:807-829.
667 Liu Z, Lv Y, Zhao N, Guan G, Wang J (2015) Protein kinase R-like ER kinase and its role in endoplasmic
668 reticulum stress-decided cell fate. Cell death & disease 6:e1822.
669 Logsdon AF, Turner RC, Lucke-Wold BP, Robson MJ, Naser ZJ, Smith KE, Matsumoto RR, Huber JD, Rosen
670 CL (2014) Altering endoplasmic reticulum stress in a model of blast-induced traumatic brain
671 injury controls cellular fate and ameliorates neuropsychiatric symptoms. Frontiers in cellular
672 neuroscience 8.
673 Ma T, Trinh MA, Wexler AJ, Bourbon C, Gatti E, Pierre P, Cavener DR, Klann E (2013) Suppression of
674 eIF2alpha kinases alleviates Alzheimer's disease-related plasticity and memory deficits. Nature
675 neuroscience 16:1299-1305.
676 Marciniak SJ, Garcia-Bonilla L, Hu J, Harding HP, Ron D (2006) Activation-dependent substrate
677 recruitment by the eukaryotic translation initiation factor 2 kinase PERK. The Journal of cell
678 biology 172:201-209.
679 Mir S, Sen T, Sen N (2014) Cytokine-Induced GAPDH Sulfhydration Affects PSD95 Degradation and
680 Memory. Molecular cell 56:786-795.
681 Moreno JA, Halliday M, Molloy C, Radford H, Verity N, Axten JM, Ortori CA, Willis AE, Fischer PM, Barrett
682 DA, Mallucci GR (2013) Oral treatment targeting the unfolded protein response prevents
683 neurodegeneration and clinical disease in prion-infected mice. Science translational medicine
684 5:206ra138.
685 Nelson CD, Kim MJ, Hsin H, Chen Y, Sheng M (2013) Phosphorylation of threonine-19 of PSD-95 by GSK-
686 3beta is required for PSD-95 mobilization and long-term depression. The Journal of
687 neuroscience : the official journal of the Society for Neuroscience 33:12122-12135.
688 Nortje J, Menon DK (2004) Traumatic brain injury: physiology, mechanisms, and outcome. Current
689 opinion in neurology 17:711-718.
690 O'Connor T, Sadleir KR, Maus E, Velliquette RA, Zhao J, Cole SL, Eimer WA, Hitt B, Bembinster LA,
691 Lammich S, Lichtenthaler SF, Hebert SS, De Strooper B, Haass C, Bennett DA, Vassar R (2008)
692 Phosphorylation of the translation initiation factor eIF2alpha increases BACE1 levels and
693 promotes amyloidogenesis. Neuron 60:988-1009.
694 Ohno M (2014) Roles of eIF2α kinases in the pathogenesis of Alzheimer's disease. Frontiers in molecular
695 neuroscience 7.
696 Park K, Biederer T (2013) Neuronal adhesion and synapse organization in recovery after brain injury.
697 Future neurology 8:555-567.
698 Pereira C, #xe1, F. uM (2013) Crosstalk between Endoplasmic Reticulum Stress and Protein Misfolding in
699 Neurodegenerative Diseases. ISRN Cell Biology 2013:22.

700 Radford H, Moreno JA, Verity N, Halliday M, Mallucci GR (2015) PERK inhibition prevents tau-mediated
701 neurodegeneration in a mouse model of frontotemporal dementia. Acta neuropathologica
702 130:633-642.
703 Rondina C, Videtta W, Petroni G, Lujan S, Schoon P, Mori LB, Matkovich J, Carney N, Chesnut R (2005)
704 Mortality and morbidity from moderate to severe traumatic brain injury in Argentina. The
705 Journal of head trauma rehabilitation 20:368-376.
706 Rubovitch V, Barak S, Rachmany L, Goldstein RB, Zilberstein Y, Pick CG (2015) The neuroprotective effect
707 of salubrinal in a mouse model of traumatic brain injury. Neuromolecular medicine 17:58-70.
708 Saito A, Ochiai K, Kondo S, Tsumagari K, Murakami T, Cavener DR, Imaizumi K (2011) Endoplasmic
709 reticulum stress response mediated by the PERK-eIF2(alpha)-ATF4 pathway is involved in
710 osteoblast differentiation induced by BMP2. The Journal of biological chemistry 286:4809-4818.
711 Schaffer DJ, Tunc-Ozcan E, Shukla PK, Volenec A, Redei EE (2010) Nuclear orphan receptor Nor-1
712 contributes to depressive behavior in the Wistar-Kyoto rat model of depression. Brain research
713 1362:32-39.
714 Sen N, Snyder SH (2011) Neurotrophin-mediated degradation of histone methyltransferase by S-
715 nitrosylation cascade regulates neuronal differentiation. Proceedings of the National Academy
716 of Sciences of the United States of America 108:20178-20183.
717 Sen N, Paul BD, Gadalla MM, Mustafa AK, Sen T, Xu R, Kim S, Snyder SH (2012) Hydrogen sulfide-linked
718 sulfhydration of NF-kappaB mediates its antiapoptotic actions. Molecular cell 45:13-24.
719 Sen N, Hara MR, Kornberg MD, Cascio MB, Bae BI, Shahani N, Thomas B, Dawson TM, Dawson VL,
720 Snyder SH, Sawa A (2008) Nitric oxide-induced nuclear GAPDH activates p300/CBP and mediates
721 apoptosis. Nature cell biology 10:866-873.
722 Sen N, Hara MR, Ahmad AS, Cascio MB, Kamiya A, Ehmsen JT, Agrawal N, Hester L, Dore S, Snyder SH,
723 Sawa A (2009) GOSPEL: a neuroprotective protein that binds to GAPDH upon S-nitrosylation.
724 Neuron 63:81-91.
725 Sen T, Sen N (2016) Treatment with an activator of hypoxia-inducible factor 1, DMOG provides
726 neuroprotection after traumatic brain injury. Neuropharmacology 107:79-88.
727 Stranahan AM, Khalil D, Gould E (2007) Running induces widespread structural alterations in the
728 hippocampus and entorhinal cortex. Hippocampus 17:1017-1022.
729 Tao X, Finkbeiner S, Arnold DB, Shaywitz AJ, Greenberg ME (1998) Ca2+ influx regulates BDNF
730 transcription by a CREB family transcription factor-dependent mechanism. Neuron 20:709-726.
731 Trinh MA, Kaphzan H, Wek RC, Pierre P, Cavener DR, Klann E (2012) Brain-specific disruption of the
732 eIF2alpha kinase PERK decreases ATF4 expression and impairs behavioral flexibility. Cell reports
733 1:676-688.
734 Truettner JS, Hu B, Alonso OF, Bramlett HM, Kokame K, Dietrich WD (2007) Subcellular stress response
735 after traumatic brain injury. Journal of neurotrauma 24:599-612.
736 Uchida M, Enomoto A, Fukuda T, Kurokawa K, Maeda K, Kodama Y, Asai N, Hasegawa T, Shimono Y,
737 Jijiwa M, Ichihara M, Murakumo Y, Takahashi M (2006) Dok-4 regulates GDNF-dependent
738 neurite outgrowth through downstream activation of Rap1 and mitogen-activated protein
739 kinase. Journal of cell science 119:3067-3077.
740 Uchida S, Hara K, Kobayashi A, Funato H, Hobara T, Otsuki K, Yamagata H, McEwen BS, Watanabe Y
741 (2010) Early life stress enhances behavioral vulnerability to stress through the activation of
742 REST4-mediated gene transcription in the medial prefrontal cortex of rodents. The Journal of
743 neuroscience : the official journal of the Society for Neuroscience 30:15007-15018.
744 Vattem KM, Wek RC (2004) Reinitiation involving upstream ORFs regulates ATF4 mRNA translation in
745 mammalian cells. Proceedings of the National Academy of Sciences of the United States of
746 America 101:11269-11274.

747 Vorhees CV, Williams MT (2006) Morris water maze: procedures for assessing spatial and related forms
748 of learning and memory. Nature protocols 1:848-858.
749 Wang Z, Iwasaki M, Ficara F, Lin C, Matheny C, Wong SH, Smith KS, Cleary ML (2010) GSK-3 promotes
750 conditional association of CREB and its coactivators with MEIS1 to facilitate HOX-mediated
751 transcription and oncogenesis. Cancer cell 17:597-608.
752 Wek RC, Cavener DR (2007) Translational control and the unfolded protein response. Antioxidants &
753 redox signaling 9:2357-2371.
754 Wu K, Meyers CA, Bennett JA, King MA, Meyer EM, Hughes JA (2004) Polyethylenimine-mediated NGF
755 gene delivery protects transected septal cholinergic neurons. Brain research 1008:284-287.
756 Zhang P, McGrath B, Li S, Frank A, Zambito F, Reinert J, Gannon M, Ma K, McNaughton K, Cavener DR
757 (2002) The PERK eukaryotic initiation factor 2 alpha kinase is required for the development of
758 the skeletal system, postnatal growth, and the function and viability of the pancreas. Molecular
759 and cellular biology 22:3864-3874.

760

761 **Acknowledgement**: We would like to acknowledge NIH funding support (RO1NS094516 and
762 RO1EY025622) for providing support to N.S, and R.G. We would also like to thank Dr. Alexis Stranahan
763 from the Augusta University for providing generous help to carryout DiI staining to study the synaptic
764 morphology.

Figure 1

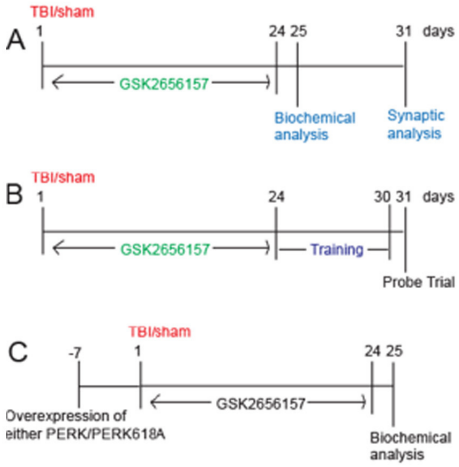

Figure 2

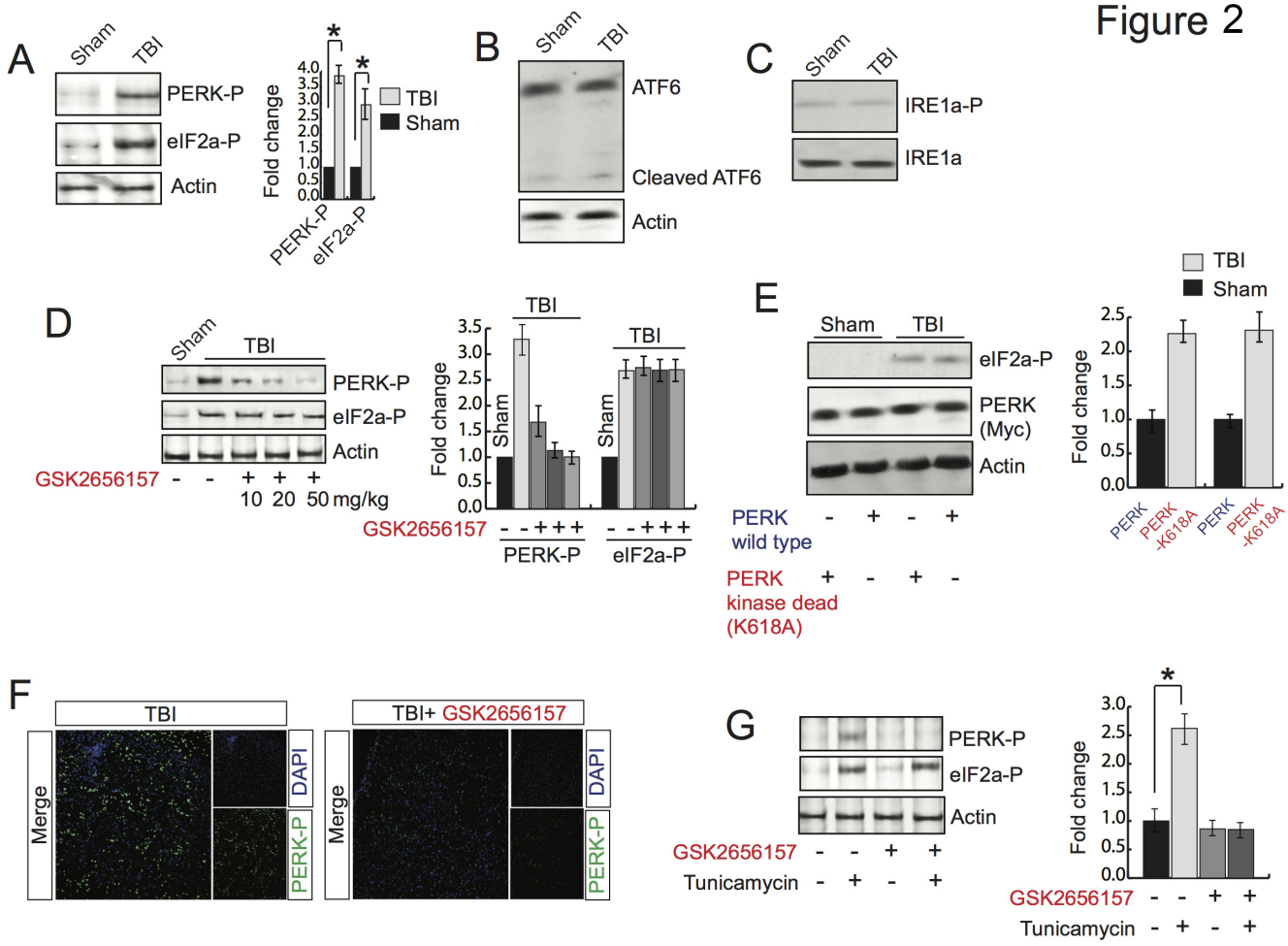

Figure 3

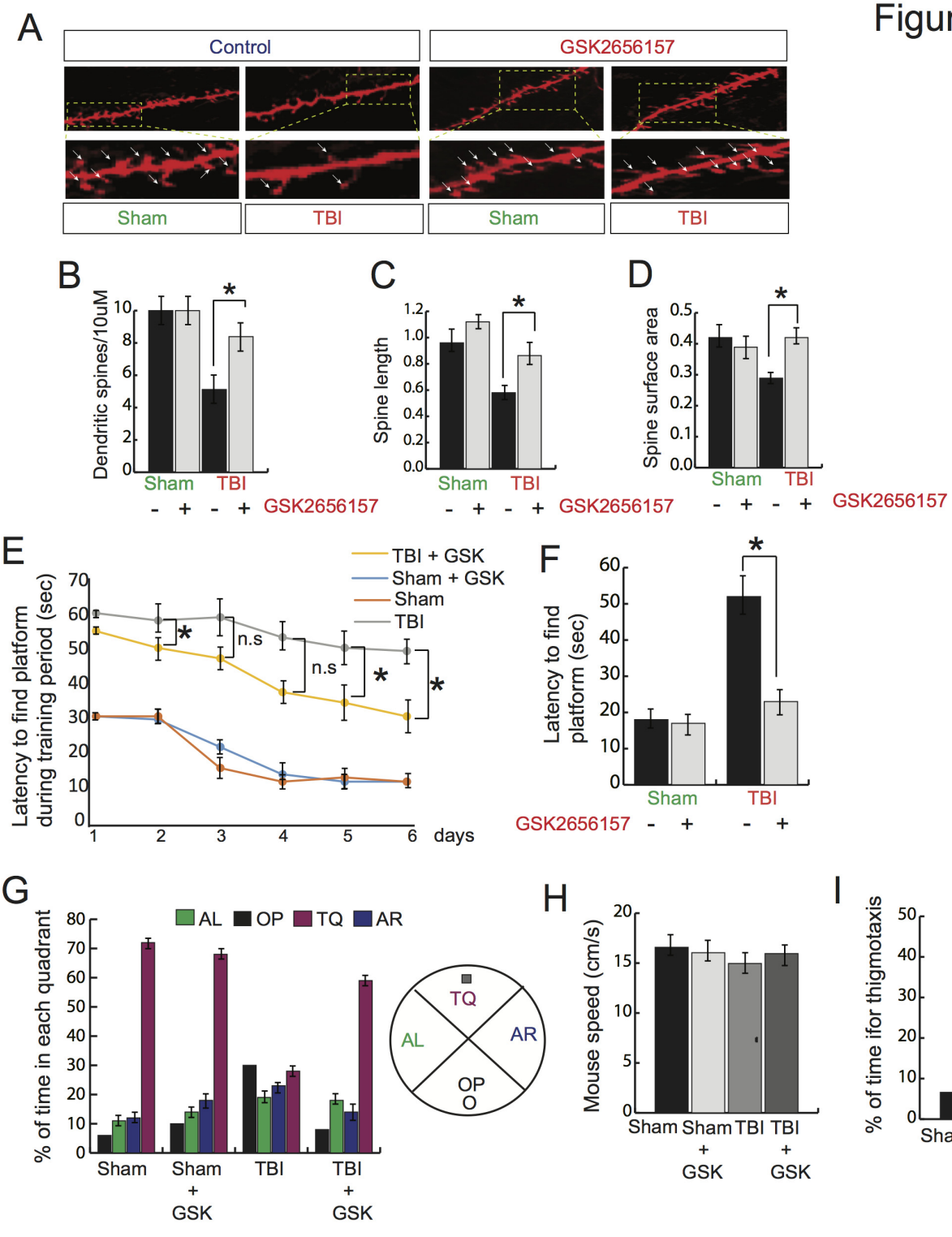

Figure 4

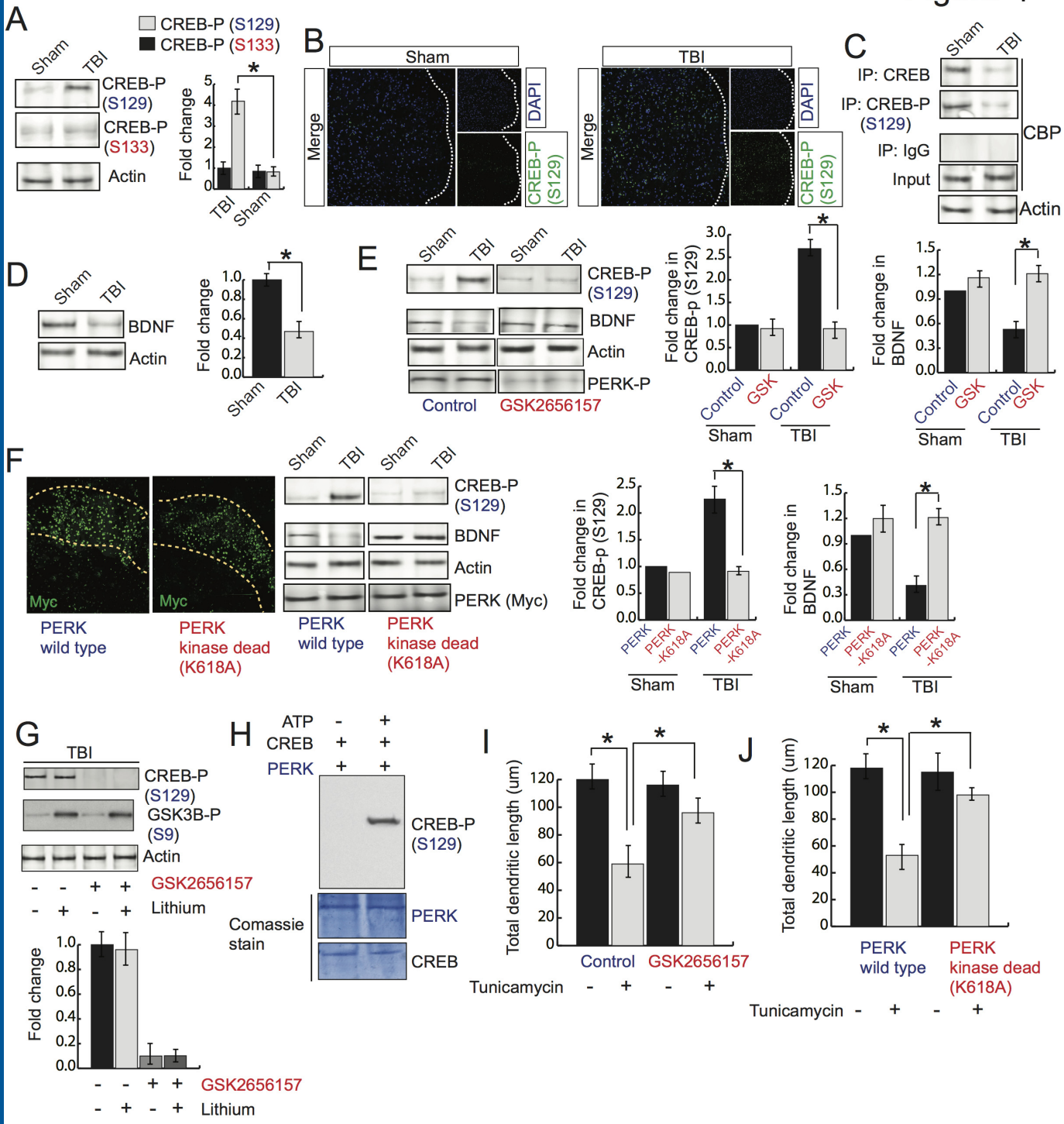

Figure 4